International Journal of Control and Automation
Vol.7, No.2 (2014), pp.309-326
http://dx.doi.org/10.14257/ijca.2014.7.2.28

The Nonlinear Modeling and Control movement of a Human Forearm for Prosthetic Applications

Gamal A. Elnashar

Automatic Control Centre, School of Engineering-Egyptian Armed Forces, 15 Yassien Raghb St., Nasr City, Cairo, Egypt

enjygamal@gmail.com

Abstract

The model and control of a human forearm is analyzed. In this work, we study the problem of human hand control carrying a mass. The equation of motion and the natural frequency of the forearm for small angular displacement are derived. We develop new methods that use vector fields in the controller construction for a set of nonlinear dynamical systems. The paper deals with compensate of non-linear system which has a similar idea as the method mentioned in linear system. The nonlinear control design procedure, as in the case of linear systems, involves three steps. The first step is the devise of a state-feedback control law, the second step involves the design of a state estimator, and the third step merges the first two steps to obtain a collective controller–estimator compensator. We have managed to design a control law for the non-linear representation of a system, in such a way that the representation of a closed loop system is affine, controllable, and observable and a closed loop system is asymptotically stable. Throughout any motion, the forearm can be considered a one-link robot manipulator which could be exploited to benefit people with disabilities (missing extremities).

Keywords: *Forearm; Nonlinear Control; Modeling; Observer, Vector Field; Lie Derivatives*

1. Introduction

The problems associated with the design of artificial arm replacements are far more challenging than those associated with the design of robotic arms or terminal devices. The design of artificial arms is a multidisciplinary effort. The design team needs an understanding of the mechanics of mechanisms, such as gears, levers, and points of mechanical advantage, and electromechanical design, such as switches, dc motors, and electronics [1]. When the someone wants to move the arm, the brain sends signals that first bond the chest muscles, which send an electrical signal to the prosthetic arm, instructing it to reposition. The procedure requires no more aware effort than it would for a person who has a ordinary arm. Typically, a person with a prosthetic arm can make only a few motions, often so slowly that many people use the arms only for limited activities. There is a separate motor for each movement. By far the most common actuator for electrically powered prostheses is the permanent magnet dc electric motor with some form of transmission [2]. In proportional control, the amount/intensity of a controlled output variable is directly related (proportional) to the amount of the input signal. For example, the output speed of a dc motor is proportional to the amount of voltage applied to its terminals. This is why dc motors are said to be speed controlled. This is also the reason why most of today's commercially available prosthetic

ISSN: 2005-4297 IJCA

components are speed controlled—it is simple [3]. Output speed is proportional to the amount of input signal. Proportional control is used where a graded response to a graded input is required. In position control the position of the prosthetic joint is proportional to the input amount/intensity. The input amount/intensity might be the position of another physiological joint or a force level. If the position of another joint is used as the input then the system is known as a position actuated, position servomechanism. If the amount of force applied by some body part is the input, then the system is a force actuated, position servomechanism [4].

With position control the amputee's ability to perceive and control prosthesis position is directly determined by his or her ability to perceive and control the input signal. A major disadvantage of position control is that, unlike velocity control, it must maintain an input signal to hold an output level other than zero. This means that power must be continuously supplied to the component to maintain a commanded position other than zero. This is one of the reasons why speed or velocity control is the dominant mode of control in externally-powered prosthetics today, despite the fact that it has been shown that position control for positioning of the terminal device in space is superior to velocity control. In control theory, a state observer is a system that provides an estimate of the internal state of a given real system, from measurements of the input and output of the real system [6]. It is typically computer-implemented, and provides the basis of many practical applications. Knowing the system state is necessary to solve many control theory problems; for example, stabilizing a system using state feedback. In most practical cases, the physical state of the system cannot be determined by direct observation. Instead, indirect effects of the internal state are observed by way of the system outputs. If a system is observable, it is possible to fully reconstruct the system state from its output measurements using the state observer. In this day of digital circuits and microprocessor based controllers pulse width modulation is the preferred method of supplying a graded (proportional) control signal to a component. A PWM stream only requires a single digital output line and a counter on the microprocessor to be implemented, whereas a conventional analog signal (linear dc voltage level) requires a full digital-to-analog (D/A) converter. PWM techniques are used extensively in switched-mode power supply design and audio amplifiers and as such, there is a large array of resources available to the designer to choose from [8].

In this study, a model for a forearm performing a motion is presented, using a new controller technique based on vector fields. Furthermore, we evaluated three position controllers. The forearm bar of mass m_1 and length b is shown in Figure 1. A mass m_2 is carried by the angular of the forearm of a human hand. During motion, the forearm can be considered to rotate about the joint (pivot point O) with muscle forcers modeled in the form of a force by triceps $\left(c_1 x^{\bullet}\right)$ and a force in biceps $\left(-c_2\theta\right)$, where c_1 and c_2 are constant and $x^{\bullet}$ is the velocity with which triceps are stretched (or contracted). We will derive the equation of motion and natural frequency of the forearm of the forearm for small angular displacement θ. The paper is organized as follows: section 1 describes an introduction about prosthetic research and its control techniques. In Section 2 the mathematical model of a human forearm is described i.e. equation of motion for the angular motion of the forearm about the pivot point O is derived, and the motion of the robot arm by a DC motor via a gear is resulting Section 3 develops a method for constructing state-feedback stabilizing controls law for a class of dynamical systems where position control algorithms are treated. Sections 4 and 5 nonlinear state-feedback controller and asymptotic state estimator are derived respectively for one-link manipulator model. Nonlinear combined controller-estimator compensator is simulated in Section 6 and Finally, A short conclusion in Section 7 summarizes the study.

2. Mathematical Modeling

Equation of motion for the angular motion of the forearm about the pivot point O [9]:

$$I_0\ddot{\theta}_P + m_2 gb\cos\theta_P + m_1 g\frac{b}{2}\cos\theta_P - F_2 a_2 + F_1 a_1 = 0 \tag{1}$$

Where θ_P the angular displacement of the forearm is, I_0 is the mass of inertia of the forearm and the mass carried:

$$I_0 = m_2 b^2 + \frac{1}{3}b^2 m_1 \tag{2}$$

And the forces in the biceps and triceps muscles ($(F_2$ and $F_1)$ are given by

$$F_2 = -c_2\theta_P \tag{3}$$

$$F_1 = c_1\dot{x} = c_1 a_1\dot{\theta}_P \tag{4}$$

Where the linear velocity of the triceps can be expressed as

$$\dot{x} \approx a_1\dot{\theta}_P \tag{5}$$

Using Equations (2)-(4), equation (1) can be rewritten as

$$I_0\ddot{\theta}_P + \left(m_2 gb + \frac{1}{2}m_1 gb\right)\cos\theta_P + c_2 a_2\theta_P + c_1 a_1^2\dot{\theta}_P = 0 \tag{6}$$

Let the forearm undergo small angular displacement (θ) about the static equilibrium position, $\bar{\theta}$, so that

$$\theta_P = \bar{\theta} + \theta \tag{7}$$

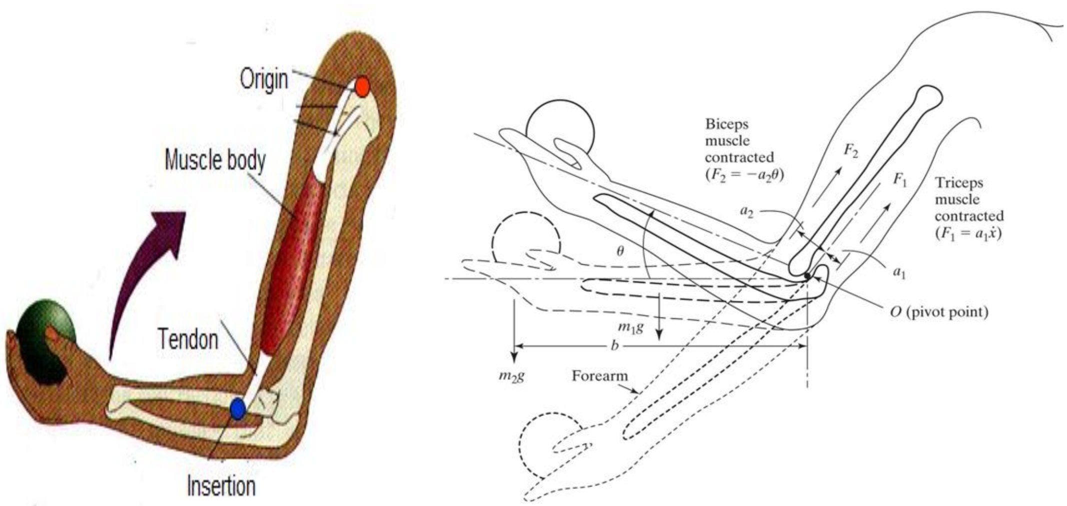

Figure 1. Forearm of a human hand carrying a mass

Using Taylor's series expansion of $\cos\theta_P$ about $\bar{\theta}_P$, the static equilibrium position, can be expressed as (for small value of θ)

$$\cos\theta_P = \cos\left(\bar{\theta}+\theta\right) \approx \cos\bar{\theta} - \theta\sin\bar{\theta} \tag{8}$$

Using $\theta_P^{\bullet\bullet} = \theta^{\bullet\bullet}$ and $\theta_P^{\bullet} = \theta^{\bullet}$, Equation (6) can be expresses as

$$I_0\theta_P^{\bullet\bullet} + \left(m_2gb + \frac{1}{2}m_1gb\right)\left(\cos\bar{\theta} - \sin\bar{\theta}\ \theta\right) + c_2a_2\left(\bar{\theta}+\theta\right) + c_1a_1^2\theta^{\bullet} = 0 \qquad \text{Or}$$

$$I_0\theta^{\bullet\bullet} + \left(m_2gb + \frac{1}{2}m_1gb\right)\cos\bar{\theta} - \sin\bar{\theta}\left(m_2gb + \frac{1}{2}m_1gb\right)\theta + c_2a_2\bar{\theta} + c_2a_2\theta + c_1a_1^2\theta^{\bullet} = 0 \tag{9}$$

Notice that the static equilibrium equation of the forearm at $\theta_P = \bar{\theta}$, Eq.(6) is given by

$$\left(m_2gb + \frac{1}{2}m_1gb\right)\cos\bar{\theta} + c_2a_2\bar{\theta} = 0 \tag{10}$$

In view of Equation (10), Equation (9) becomes

$$\left(m_2b^2 + \frac{1}{3}b^2m_1\right)\theta^{\bullet\bullet} + c_1a_1^2\theta^{\bullet} + \left\{c_2a_2 - \sin\bar{\theta}\ gb\left(m_2 + \frac{1}{2}m_1\right)\right\}\theta = 0 \tag{11}$$

which denotes the equation of motion of the forearm.

The undamped natural frequency of the forearm can be expressed as:

$$\omega_n = \sqrt{\frac{c_2a_2 - \sin\bar{\theta}\ gb\left(m_2 + \frac{1}{2}m_1\right)}{b^2\left(m_2 + \frac{1}{3}m_1\right)}} \tag{12}$$

The design of fully functioning artificial arms with physiological speeds-of- response and strength (or better) that can be controlled almost without thought is the goal of upper extremity prosthetics research. Unfortunately, current prosthetic components and interface techniques are still a long way from realizing this goal [1]. By far the most common actuator for electrically powered prostheses is the permanent magnet dc electric motor with some form of transmission. While there is much research into other electrically powered actuator technologies, such as shape memory alloys and electro active polymers, none is to the point where it can compete against the dc electric motor.

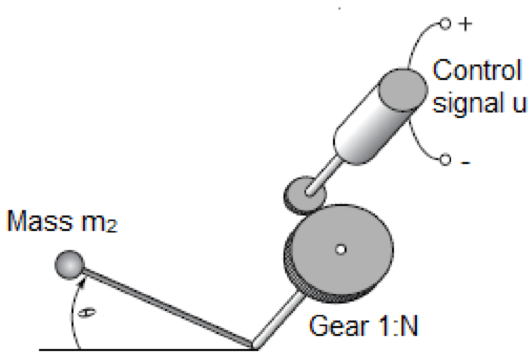

Figure 2. A manipulator of length b_1 and mass m_1 controlled by a DC motor via a gear.

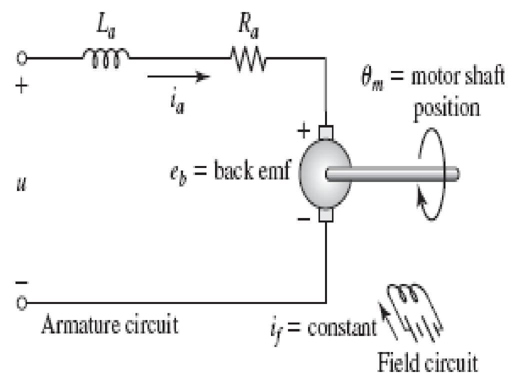

Figure 3. Schematic of an armature controlled DC-Motor

In terms of artificial arm, consider a model of one-link robot manipulator shown in Figure 2. Many different types of drive mechanisms have been devised to allow wrist and forearm drive motors and gearboxes to be mounted close to the first and second axis of rotation, thus minimizing the extended mass of the arm. The motion of the robot arm is controlled by a DC motor via a gear [10]. The DC motor is armature-controlled and its schematic is shown in Figure 3.The torque delivered by the motor is: $T_m = K_m i_a$, where k_m is the motor-torque constant, and i_a is the armature current. Let N denote the gear ratio. Then we have $\frac{\theta_P}{\theta_m} = \frac{radius\ of\ motor\ gear}{radius\ of\ \text{arm}\ gear} = \frac{Number\ of\ teeth\ motor\ gear}{Number\ of\ teeth\ arm\ gear} = \frac{1}{N}$

The work done by gears are proportional to their number of teeth and the work done by the gears must be equal. Let T_P denote the torque applied to the robot arm. Then,

$T_P \theta_P = T_m \theta_m$. Thus, the torque applied the rod is $T_P = NT_m = NK_m i_a$. We use Newton's second law to write the equation modeling the arm dynamics,

$$\left(m_2 b^2 + \frac{1}{3} b^2 m_1 \right) \ddot{\theta}_P = \left(m_2 gb + \frac{1}{2} m_1 gb \right) \cos \theta_P + NK_m i_a \tag{13}$$

Where g=9.8 m/sec^2 is the gravitational constant. Applying Kirchhoff's voltage law to the armature circuit yields

$$L_a \frac{di_a}{dt} + R_a i_a + k_b N \frac{d\theta_P}{dt} = u \tag{14}$$

Where k_P is the back *emf* constant. We can now construct a third-order state-space model of the one-link robot. For this we choose the following state variables:

$$x_1 = \theta_P, x_2 = \frac{d\theta_P}{dt} = \omega_P, x_3 = i_a,$$

Then, the model in state-space format is

$$\begin{bmatrix} \dot{x}_1 \\ \dot{x}_2 \\ \dot{x}_3 \end{bmatrix} = \begin{bmatrix} x_2 \\ \dfrac{\left(m_2 gb + \frac{1}{2} m_1 gb\right)}{\left(m_2 b^2 + \frac{1}{3} b^2 m_1\right)} \cos x_1 + \dfrac{N k_m}{\left(m_2 b^2 + \frac{1}{3} b^2 m_1\right)} x_3 \\ -\dfrac{k_b N}{L_a} x_2 - \dfrac{R}{L_a} x_3 \end{bmatrix} + \begin{bmatrix} 0 \\ 0 \\ \dfrac{1}{L_a} \end{bmatrix} u \;, \tag{15}$$

Reasonable parameters of the robot are: m_2*=5kg*, m_1*=2kg*, *b=30cm*, *N=10*, k_m*=0.1Nm/A*, k_b*=0.1 V sec/rad*, R_a*=1Ω*, L_a*=100mH*. Then the robot model takes the form:

$$\begin{bmatrix} \dot{x}_1 \\ \dot{x}_2 \\ \dot{x}_3 \end{bmatrix} = \begin{bmatrix} x_2 \\ 34.59 \cos x_1 + 1.96 x_3 \\ -10 x_2 - 10 x_3 \end{bmatrix} + \begin{bmatrix} 0 \\ 0 \\ 10 \end{bmatrix} u \tag{16}$$

We assume that the output y, is

$$y = x_1 \tag{17}$$

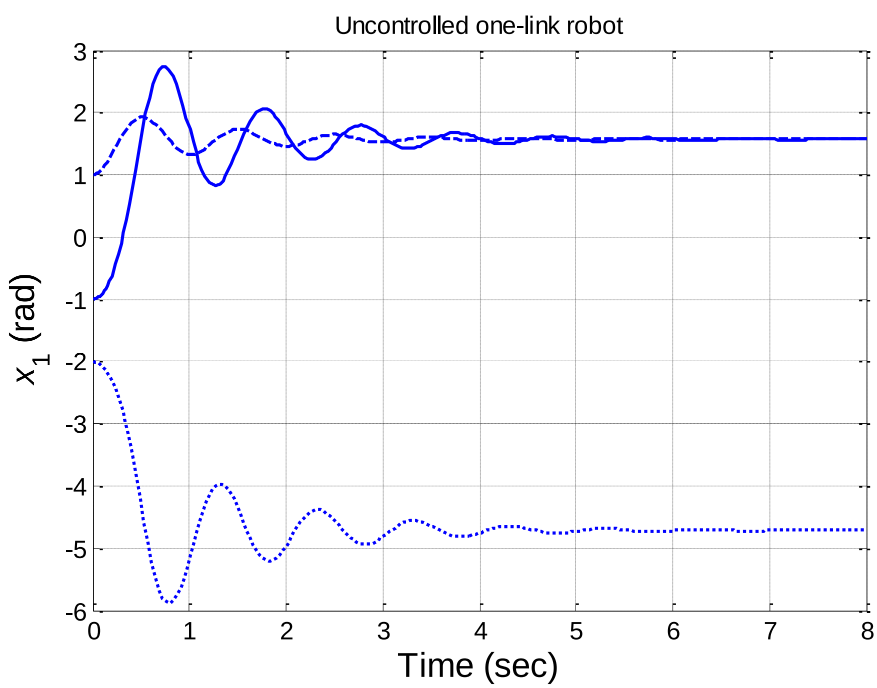

Figure 4. Plots of the one-link manipulator's, versus time for three different initial angles $\theta(0)$

Time histories of state trajectories of the uncontrolled nonlinear system of the model by (16) and (17) $[x_1(t)=\theta(t)]$ versus time is shown in Figure 4. The manipulator is driven by $u=0$, initial conditions $x_1(0)=1,-1\ and\ -2$ and $x_2(0)=0$ and $x_3(0)=0$. It is clear that drastic change response due to the initial conditions and also the system has more than one equilibrium points.

3. Nonlinear Control

One of the objective of this paper is to devise a method for constructing state-feedback stabilizing control law for a class of dynamical nonlinear systems modeled by

$$\begin{aligned} x^{\bullet} &= f(x)+G(x)u, \\ y &= h(x) \end{aligned} \tag{18}$$

where $f:R^n \to R^n, G:R^n \to R^{nxm}$ and the output map $h:R^n \to R^p$

We thus first discuss a method for reducing a nonlinear system model into an equivalent form that is a generalization of the controller form known from linear system theory. In our subsequent discussion, we will be using three types of *Lie derivatives* [11, 12]. They are as follows:

1. Derivative of a vector field with respect to a vector field, also known as the Lie bracket.

Given the vector-valued functions $f:R^n \to R^n$ and $g:R^n \to R^n$, where f and g are C^{∞} vector fields, their Lie bracket is defined as

$$[f,g]=\frac{\partial f}{\partial x}g-\frac{\partial g}{\partial x}f \tag{19}$$

2. Derivative of a function with respect to a vector field. Let $let\ h:\mathrm{R}^n \to \mathrm{R}$ be a C^{∞} function on R^n. Let $Dh=\nabla h^T$, where ∇h is the gradient (a column vector) of h with respect to x. Then, the Lie derivative of the function h with respect to the vector field f, denoted $L_f h\ or\ L_f(h)$, is defined as

$$L_f h = L_f(h)=\langle \nabla h, f\rangle = Dh\ f = \frac{\partial h}{\partial x_1}f_1+\frac{\partial h}{\partial x_1}f_1+\cdots+\frac{\partial h}{\partial x_n}f_n \tag{20}$$

3. *Derivative of* Dh *with respect to the vector field.* The Lie derivative of Dh with respect to the vector field f, denoted $L_f(Dh)$, is defined as

$$L_f(Dh)=\left(\frac{\partial \nabla h}{\partial x}f\right)^T + Dh\frac{\partial f}{\partial x}=DL_f h=\nabla L_f^T h \tag{21}$$

Our goal now is to construct a C^{∞} state variable transformation $z=T(x),\ T(0)=0$

for which there is a C^{∞} inverse $x=T^{-1}(z)$, such that system model $x^{\bullet}=f(x)+g(x)u$ in the new coordinates has the form

$$\begin{bmatrix} \dot{z}_1 \\ \dot{z}_2 \\ \vdots \\ \dot{z}_{n-1} \\ \dot{z}_n \end{bmatrix} = \begin{bmatrix} z_2 \\ z_3 \\ \vdots \\ z_n \\ \bar{f}_n(z_1, z_2, \cdots, z_n) \end{bmatrix} + \begin{bmatrix} 0 \\ 0 \\ \vdots \\ 0 \\ 1 \end{bmatrix} u \tag{22}$$

A transformation $z = T(x)$ such that $T(0) = 0$ and for which there is a C^{∞} inverse $\boldsymbol{x} = \boldsymbol{T}^{-1}(\boldsymbol{z})$ is called a *diffeomorphism*[13]. The transformation $z = T(x)$ has the form

$$T = \left[T_1, L_f T_1, \cdots, L_f^{n-2} T_1, L_f^{n-1} T\right]^T \tag{23}$$

The above means that the problem of constructing the desired transformation $z = T(x)$ is reduced to finding its first component T_1. The remaining components of $\boldsymbol{T}$ can be successively computed using T_1. The row vector $\frac{\partial T_1(x)}{\partial x}$ is the last row of the inverse of the controllability matrix, provided the controllability matrix is invertible. We denote the last row of the inverse of the controllability matrix by $\boldsymbol{q(x)}$. Then, the problem we have to solve is to find $T_1 = R^n \to R$ such that $\frac{\partial T_1(x)}{\partial x} = q(x),\ T_1(0) = 0$

where the controllability matrix of the nonlinear system can be expressed in terms of *Lie* brackets as:

$$Q = \left[\left(ad^0 f, g\right) \quad \left(ad^1 f, g\right) \quad \cdots \quad \left(ad^{n-1} f, g\right)\right] \tag{24}$$

The controllability matrix of the system model in Equations (16, 17) is

$$Q = \left[\left(ad^0 f, g\right) \quad \left(ad^1 f, g\right) \quad \left(ad^2 f, g\right)\right] = \begin{bmatrix} 0 & 0 & 19.6 \\ 0 & 19.6 & -196 \\ 10 & -100 & 804 \end{bmatrix} \tag{25}$$

The above controllability is of full rank on R^3. The last row of its inverse is

$q = \begin{bmatrix} 0.051 & 0 & 0 \end{bmatrix}$, Hence $T_1 = 0.05 x_1$

Having obtained T_1, we construct the desired transformation $Z = T(x)$, where

$$T(x) = \begin{bmatrix} T_1 \\ L_f T_1 \\ L_f\left(L_f T\right) \end{bmatrix} = \begin{bmatrix} 0.051 x_1 \\ 0.051 x_2 \\ 1.77 \cos x_1 + 0.1 x_3 \end{bmatrix} \tag{26}$$

Note that the inverse transformation $x = T^{-1}(z)$ exist and has the form

$$T^{-1}(z) = \begin{bmatrix} 19.6z_1 \\ 19.6z_2 \\ 10z_3 - 17.7\cos(19.6z_1) \end{bmatrix} \tag{27}$$

Further more $\dfrac{\partial T}{\partial x} = \begin{bmatrix} 0.05 & 0 & 0 \\ 0 & 0.05 & 0 \\ -1.77\sin x_1 & 0 & 0.1 \end{bmatrix}$ (28)

Applying the transformation $Z = T(x)$ to the model of the one-link robot manipulator yields

$$z^{\bullet} = \frac{\partial T}{\partial x} f(x)\Big|_{x=T^{-1}(z)} + \frac{\partial T}{\partial x} g(x)\Big|_{x=T^{-1}(z)} u$$

$$z^{\bullet} = \begin{bmatrix} z_2 \\ z_3 \\ -34z_2\sin 19.6z_1 - 19.6z_2 - 10z_3 + 17.7\cos(19.6z_1) \end{bmatrix} + \begin{bmatrix} 0 \\ 0 \\ 1 \end{bmatrix} u \tag{29}$$

4. Nonlinear State-feedback Control

Once the plant model is transformed into the controller form, we can construct a state-feedback controller in the new coordinates and then, using the inverse transformation, represent the controller in the original coordinates [14]. While constructing the controller in the new coordinates, a part of the controller is used to cancel nonlinearities, thus resulting in a linear system in the new coordinates. Then, we proceed to construct the other part of the controller. This part can be designed using linear control methods because the feedback linearized system is linear. The controller form of the one-link manipulator model is given by (29). It is easy to design a stabilizing state-feedback controller in the new coordinates. It takes the form

$$u = -\overline{f}_3(z_1, z_2, z_3) - \left(k_1 z_1 + k_2 z_2 + k_3 z_3\right), \tag{30}$$

Where $\overline{f}_3(z_1, z_2, z_3) = -34z_2\sin 19.6z_1 - 19.6z_2 - 10z_3 + 17.7\cos(19.6z_1)$

Suppose that the desired closed-loop poles of the feedback linearized one-link manipulator are to be located at $\left(-2 \pm j3.46, 8\right)$ which verify a damping factor $\zeta = 0.5$ and natural frequency $\omega_n = 4\ rad/\sec$. Then, the linear feedback gains $k_i = i = 1,2,3$ that shift the poles to these desired locations are $k_1 = 128$, $k_2 = 48$, $k_3 = 12$.

Applying (30) with the above values of the linear feedback gains to the model gives

$$z^{\bullet}=\begin{bmatrix}0 & 1 & 0\\ 0 & 0 & 1\\ -128 & -48 & -12\end{bmatrix}z \tag{31}$$

Next, applying the inverse transformation yields the controller in the original coordinates,

$$u=-6.528x_1-1.428x_2-0.2x_3-21.24\cos x_1-1.81x_2\sin x_1 \tag{32}$$

In Figure 5, three plots of the manipulator's link angle, $x_1=\theta$, versus time are presented. The initial conditions have the form $x(0)=\begin{bmatrix}\theta(0) & 0 & 0\end{bmatrix}^T$. The control law applied to the manipulator is given by (32).

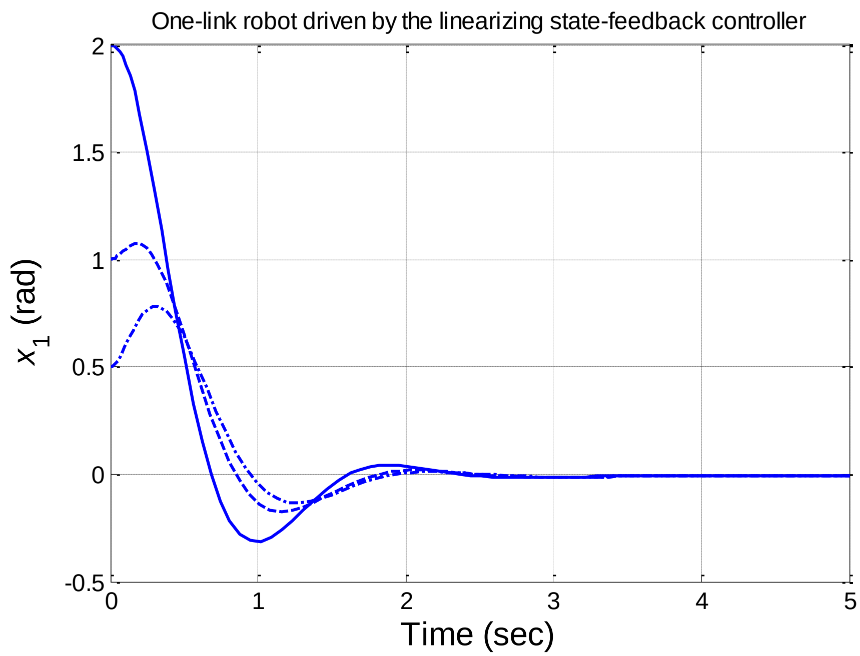

Figure 5. Plots of the one-link manipulator's link angle, $x_1=\theta$, versus time for three different initial angles $\theta(0)$. The manipulator is driven by the state-feedback control law (32)

5. Nonlinear Observer Form

In this section we discuss the problem of transforming a class of nonlinear system models into an observer form, which is then used to construct state estimators for these systems [15-17]. We consider a nonlinear system model of the form of equation (18). We desire to find a state variable transformation, written as $x=T(z)$, such that the model in the z coordinates is

$$z^{\bullet}=Az+\alpha(y)=\bar{f}(z), \qquad y=\begin{bmatrix}0 & 0 & \cdots & 0 & 1\end{bmatrix}z=cz \tag{33}$$

It is easy to verify that the state $\bar{z}$ of the dynamical system

$$\bar{z}^{\bullet} = (A - LC)\bar{z} + \alpha(y) + Ly \quad (34)$$

Will asymptotically converge to the state **z** of (33) if the matrix ***A−Lc*** is asymptotically stable.

This is because the dynamics of the error, $e = \bar{z} - z$ are described by

$$e^{\bullet} = (A - LC)e, \qquad e(t_0) = \bar{z}(t_0) - z(t_0) \quad (35)$$

Taking the derivative of $x = T(z)$ with respect to time yields

$$x^{\bullet} = \frac{\partial T}{\partial z} z^{\bullet} = \frac{\partial T}{\partial z} \bar{f}(z) \quad (36)$$

where we represent the Jacobian matrix of ***T(z)***, denoted $\frac{\partial T}{\partial z}$, as

$$\frac{\partial T}{\partial z} = DT = \left[\frac{\partial T}{\partial z_1} \quad \cdots \quad \frac{\partial T}{\partial z_n} \right] \quad (37)$$

With the help of Lie-derivative notation introduced above,

$$\frac{\partial T}{\partial z_{k+1}} = \left[f, \frac{\partial T}{\partial z_k} \right] = \left(ad^1 f, \frac{\partial T}{\partial z_k} \right), \qquad k = 1, 2, \ldots, n-1 \quad (38)$$

We express all the columns of the *Jacobian* matrix (37) of $T(z)$ in terms of the starting vector $\frac{\partial T}{\partial z_1}$, that is,

$$\frac{\partial T}{\partial z} = \left[\left(ad^0 f, \frac{\partial T}{\partial z_1} \right) \quad \left(ad^1 f, \frac{\partial T}{\partial z_1} \right) \quad \ldots \quad \left(ad^{n-1} f, \frac{\partial T}{\partial z_1} \right) \right] \quad (39)$$

To obtain an expression for the starting vector $\frac{\partial T}{\partial z_1}$, we use the output equation

$$y = h(x) = z_n \quad (40)$$

We use the chain rule when taking the partial derivative of (40) with respect to ***z*** to get

$$\frac{\partial h(x)}{\partial x} \frac{\partial T}{\partial z} = \begin{bmatrix} 0 & 0 & \ldots & 0 & 1 \end{bmatrix} \quad (41)$$

We utilize derivative of Dh with respect to the vector field to express the first component on the left-hand side of the above as

$$\frac{\partial h(x)}{\partial x}\frac{\partial T}{\partial z_1}=L_f^0\left(Dh\right)\frac{\partial T}{\partial z_1}=0 \tag{42}$$

By repeated application of the Leibniz formula and (39), we express (41) equivalently as

$$\left[L_f^0\left(Dh\right)\quad L_f^1\left(Dh\right)\quad \dots \quad L_f^{n-2}\left(Dh\right)\quad L_f^{n-1}\left(Dh\right)\right]^T\frac{\partial T}{\partial z_1}=\left[0\quad 0\quad \dots \quad 0\quad 1\right]^T \tag{43}$$

The first term of the left hand side is called *the observability matrix* of the nonlinear system model (18). It follows from (43) that the starting vector $\frac{\partial T}{\partial z_1}$ is equal to the last column of the inverse of the observability matrix. The observability matrix for the system is

$$\begin{bmatrix} L_f^0\left(Dh\right) \\ L_f^1\left(Dh\right) \\ L_f^2\left(Dh\right)\end{bmatrix}=\begin{bmatrix} 0 & 1 & 0 \\ 0 & 0 & 1 \\ -34.59\sin x_1 & 0 & 1.96\end{bmatrix} \tag{44}$$

The starting vector $\partial T/\partial z_1$ is the last column of the inverse of the above observability matrix,

$$\frac{\partial T}{\partial z_1}=\left[0\quad 0\quad 0.51\right]^T \tag{45}$$

We will now find the Jacobian matrix of the desired transformation:

$$\frac{\partial T}{\partial z}=\left[\left(ad^0 f,\frac{\partial T}{\partial z_1}\right)\quad \left(ad^1 f,\frac{\partial T}{\partial z_1}\right)\quad \left(ad^2 f,\frac{\partial T}{\partial z_1}\right)\right]=\begin{bmatrix} 0 & 0 & 1 \\ 0 & 1 & -10 \\ 0.51 & -5 & 40\end{bmatrix} \tag{46}$$

Therefore, we can take

$$x=T(z)=\begin{bmatrix} 0 & 0 & 1 \\ 0 & 1 & -10 \\ 0.51 & -5 & 40\end{bmatrix}z \quad and \quad z=T^{-1}(x)=\begin{bmatrix} 19.6 & 9.8 & 1.96 \\ 10 & 1 & 0 \\ 1 & 0 & 0\end{bmatrix}x \tag{47}$$

The system in the new coordinates has the form

$$z^{\bullet}=\left(\frac{\partial T}{\partial z}\right)^{-1} f(x)\bigg|_{x=T(z)}+\left(\frac{\partial T}{\partial z}\right)^{-1} g(x)\bigg|_{x=T(z)} u=Az+\gamma(y,u)$$

$$y=cz$$

Performing simple manipulations yields

$$z^{\bullet}=\begin{bmatrix}0&0&0\\1&0&0\\0&1&0\end{bmatrix}z+\begin{bmatrix}339.1\cos y+19.6u\\34.59\cos y-19.6y\\-10y\end{bmatrix}$$
$$y=\begin{bmatrix}0&0&1\end{bmatrix}z=z_3 \tag{48}$$

Once the nonlinear system model (18) is in the observer form, we can proceed with the construction of an asymptotic state estimator using the technique from the linear systems. The state estimator dynamics in the new coordinates are

$$\dot{\bar{z}}=\left(A-LC\right)\bar{z}+Ly+\gamma\left(y,u\right) \tag{49}$$

where the estimator gain vector $\boldsymbol{L}$ is chosen so that the matrix ***(A−Lc)*** has its eigenvalues in the desired locations in the open left-hand complex plane. It is easy to verify that the state estimation error, $z-\bar{z}$ satisfies the linear differential equation

$$\frac{d}{dt}\left(z-\bar{z}\right)=\left(A-Lc\right)\left(z-\bar{z}\right) \tag{50}$$

Applying the inverse transformation to (49), we obtain the state estimator dynamics in the original coordinates. We illustrate the above method of constructing a state estimator using the model of the one-link manipulator from the previous model. We first construct a state estimator for the one-link manipulator model in the observer form given by (48). Suppose that we wish the eigenvalues of the state estimator matrix, $\boldsymbol{A}-\boldsymbol{Lc}$, to be located at $\{-9,-10,-11\}$. Then, the estimator gain vector is L= [990 299 30]T .With the above choice of the state estimator design parameters, its dynamics in the new coordinates become

$$\dot{\bar{z}}=\begin{bmatrix}0&0&-990\\1&0&-299\\0&1&-30\end{bmatrix}\bar{z}+\begin{bmatrix}990\\299\\30\end{bmatrix}y+\begin{bmatrix}339.1\cos y+19.6u\\34.59\cos y-19.6y\\-10y\end{bmatrix},$$
$$y=\begin{bmatrix}0&0&1\end{bmatrix}z=z_3 \tag{51}$$

Using transformations (47), we represent the state estimator dynamics in the original coordinates,

$$\dot{\bar{x}}\approx\begin{bmatrix}-20&1&0\\-79.4&-0.196&1.96\\92&-9.01&-9.8\end{bmatrix}\bar{x}+\begin{bmatrix}30\\-1\\210\end{bmatrix}y+\begin{bmatrix}-10y\\34.59\cos y+80.4y\\-302y+10u\end{bmatrix}, \tag{52}$$

Performing simple manipulations, we represent the above state estimator as

$$\dot{\bar{x}} \approx \begin{bmatrix} 0 & 1 & 0 \\ 0 & 0 & 1.96 \\ 0 & -9.1 & -9.8 \end{bmatrix} \bar{x} + \begin{bmatrix} 0 \\ 34.59\cos y \\ 0 \end{bmatrix} - \begin{bmatrix} 20 \\ 79.4 \\ -92 \end{bmatrix} \left(\bar{y} - y \right) + \begin{bmatrix} 0 \\ 0 \\ 10 \end{bmatrix} u,$$

$$y = \begin{bmatrix} 1 & 0 & 0 \end{bmatrix} x = x_1 \qquad (53)$$

$$\bar{y} = \begin{bmatrix} 1 & 0 & 0 \end{bmatrix} \bar{x} = \bar{x}_1$$

6. Nonlinear Combined Controller–estimator Compensator

The designed state feedback controller is singularity free, and guarantees asymptotic tracking of smooth reference trajectories for the speed of the motor under time-varying load torque and rotor resistance uncertainty, for any initial condition [20]. Having constructed a state estimator, we use the state estimates, rather than the states themselves, in the state-feedback control law implementation. The question now is how the incorporation of the state estimator affects the stability of the closed-loop system with the combined estimator– controller compensator in the loop. Recall that in the case of linear systems, we were able to show that the closed-loop system was asymptotically stable. In the present case, one has to be careful when analyzing the stability of the closed-loop system with the combined estimator–controller compensator in the loop. The plant's nonlinearities may cause difficulties in stabilizing the closed-loop system using the combined controller–estimator compensator [21]. However, s for which the Lipschitz condition is satisfied—one should be able to find stability conditions in terms of the on linearity's Lipschitz constant and the location of the estimator's poles rather easily. We now illustrate the implementation of the combined estimator–controller compensator on the one-link manipulator model., the controller is

$$u = -6.528\bar{x}_1 - 1.428\bar{x}_2 - 0.2\bar{x}_3 - 21.24\cos\bar{x}_1 - 1.81\bar{x}_2 \sin\bar{x}_1 \qquad (54)$$

In Figure 6, plots of the one-link manipulator output for three different initial conditions are shown. The manipulator is driven by the combined controller-estimator compensator consisting of the state estimator (53) and the control law (54). The initial conditions of the estimator were set to zero while the initial conditions of the plant were the same as when we implemented the state-feedback control alone. An observer designed using Lie algebraic methods is valid in any region where a state transformation to (51) can be found. A state observer typically combines system input/output with a mathematical model to predict the behavior of that system. Estimated $x_1(t)$ versus time with compensator in the loop and zero initial conditions is shown in Figure 7. Comparing plots of Figures 5, 6 and 7, the results show that, state observer is much alike in dealing with nonlinear system. This technique is often successful for solving real-world control problems.

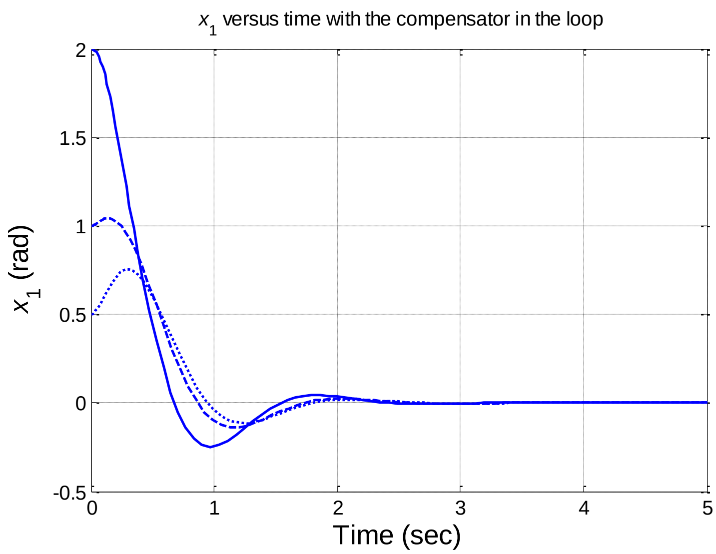

Figure 6. Plots of the one-link manipulator's link angle, $x_1 = \theta$, versus time for three different initial angles $\theta(0)$. The manipulator is driven by the combined controller–estimator compensator

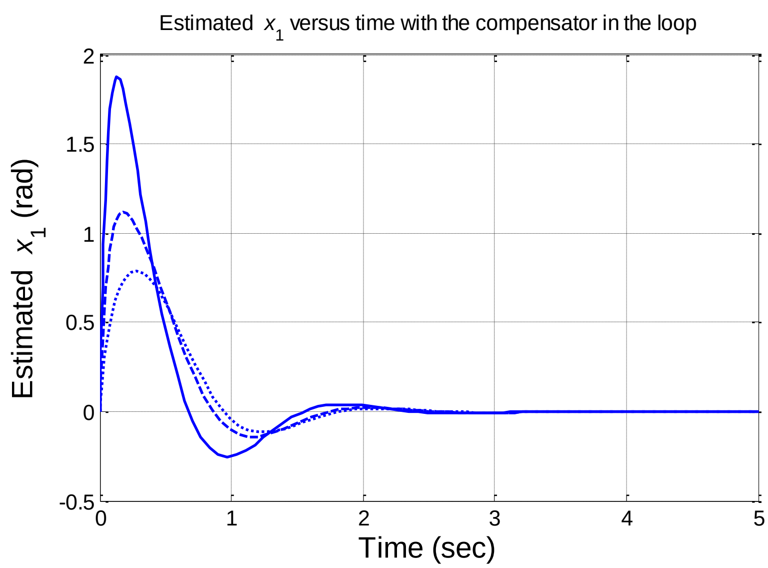

Figure 7. Plots of the one-link manipulator's link angle, $x_1 = \theta$, versus time for three different initial angles $\theta(0)$. The manipulator is driven by the combined controller–estimator compensator

7. Conclusions

An analysis and design of fully functioning artificial arms with speeds-of response and strength is conducted. The equation of motion and natural frequency of a human forearm is derived. Synthesis of control law for non-linear systems based on vector fields has been successfully solved. The method is exact and does not require any system linearization. We have managed to design a control law for the non-linear representation of a system, which is controllable and observable, in such a way that the representation of a closed loop system is affine, controllable, observable and asymptotically stable. This fact gives us more flexibility in the choice of the desired behavior of a closed loop system than a linear one. We presented an introduction to qualitative theory of a nonlinear control system, with the main emphasis on controllability and observabilty properties of such systems. We introduced the differential geometric language of vector fields and Lie bracket. We explored Lie-algebraic techniques for nonlinear observer design. The advantage of these techniques, were that they attempt to exploit our knowledge of linear observer design by reducing a nonlinear observer problem to one that can be handled by linear techniques. We illustrated our considerations with forearm nonlinear system. The combination of the nonlinear observer and the nonlinear controller stabilizes the system and guarantees exponential convergence of the tracking error to zero.

References

[1] R. F. f. Weir, “Design of artificial arms and hands for prosthetic applications”, McGraw-Hill Companies, (**2004).**

[2] R. F. f. Weir, C. W. Heckathorne and D. S. Childress, “Cineplasty as a Control Input for Externally Powered Prosthetic Components”, Journal of Rehabilitation Research and Development, vol. 38, no. 4, **(2001**) July/August, pp. 357–363.

[3] W. H. Yeadon and A. W. Yeadon, “Handbook of Small Electric Motors”, McGraw-Hill, New York, **(2001**).

[4] G. F. Franklin, J. D. Powell and A. Emami-Naeini, “Feedback Control of Dynamic Systems (5th ed.)”, Pearson Prentice Hall, Upper Saddle River, NJ**, (2006).**

[5] G. J. Bakker and H. Nijmeijer, “Comments on Control design for multivariable nonlinear time-varying systems”, International Journal of Control, vol. 41, no. 6, **(1985**), pp. 1627–1629.

[6] N. S. Nise, “Control Systems Engineering (3rd ed.)”, Wiley, New York, (**2000**).

[7] K. Ogata, “System Dynamics (4th ed.)”, Pearson Prentice Hall, Upper Saddle River, NJ, (**2004**).

[8] C. Altafini, “Geometric Control Methods for Nonlinear Systems and Robotic Applications”, Doctoral Thesis, Stockholm, (**2001)** May.

[9] S. S. Rao, “Mechanical vibrations”, 5th ed., Prentice Hall Upper Saddle River, NJ, (**2011).**

[10] A. Isidori, “Nonlinear Control Systems”, third edition, Springer-Verlag, London, **(1995).**

[11] R. Marino and P. Tomei, “Nonlinear Control Design: Geometric, Adaptive and Robust”, Prentice-Hall Europe, London**, (1995).**

[12] R. Su, “On the linear equivalents of nonlinear systems”, Systems & Control Letters, vol. 2, no. 1, (**1982)** July, pp. 48–52.

[13] L. R. Hunt, R. Su and G. Meyer, “Global transformations of nonlinear systems”, IEEE Transactions on Automatic Control, vol. AC-28, no. 1, (**1983**) January, pp. 24–31.

[14] S. H. ˙ Zak and C. A. MacCarley, “State-feedback control of non-linear systems”, International Journal of Control, vol. 43, no. 5, (**1986**), pp. 1497–1514.

[15] D. Bestle and M. Zeitz, “Canonical form observer design for non-linear time-variable systems”, International Journal of Control, vol. 38, no. 2, (**1983)**, pp. 419–431.

[16] M. Zeitz, “Comments on Comparative study of non-linear state-observation techniques”, International Journal of Control, vol. 46, no. 5, (**1987)**, pp. 1861–1863.

[17] B. L. Walcott, M. J. Corless and S. H. Zak, “Comparative study of non-linear state-observation techniques”, International Journal of Control, vol. 45, no. 6, **(1987)**, pp. 2109-2132.

[18] D. Bestle and M. Zeitz, “Canonical form observer design for non-linear time-variable systems”, International Journal of Control, vol. 38, no. 2, (**1983)**, pp. 419-431.

[19] A. Mesbaha, A. E. M. Huesmana, H. J. M. Kramerb and P. M. J. Van den Hofa, “A comparison of nonlinear observers for output feedback model-based control of seeded batch crystallization processes”, Journal of Process Control, vol. 21, (**2011)**, pp. 652–666.

[20] A. Ebrahim and G. Murphy, “Adaptive backstepping control of an induction motor under time-varying load torque and rotor resistance uncertainty”, Int. J. of Automation and Control, vol. 2, no. 4, (**2008)**, pp. 401-417.

[21] F. A. Pintara and N. Yoganandana, “Dynamic Bending Tolerance of the Human Forearm”, Traffic Injury Prevention, vol.3, no. 1, (**2002**), pp. 43-48.

Author

Gamal A. Elnashar was born in Dakhliah-Egypt on February 17, 1965. In 1988 he received his B.Sc. degree from the department of electrical engineering. His MSc. Degree in the field of automatic control from Military Technical Collage (MTC)-Egypt in 1994. He received his Ph. D. degree from the department of electrical and computer engineering from the Catholic University of America- Washington D. C. in 2000. He has been serving on the MTC research faculty since the year 2000 in the areas of identification, design, and control engineering systems. He worked as a visiting scholar in Virginia Tech.-Blacksburg in 2008. He has authored several reports and papers on data acquisition systems, sensors and automatic control-related short courses at MTC.

